Journal of Inclusion Phenomena and Macrocyclic Chemistry **34:** 167–185, 1999.

Structure and Kinetics of Desolvation of 2-Hexanone Inclusion Compounds of the Hexapedal Hosts, Hexakis(3-hydroxy-3,3-diphenyl-2-propynyl)benzene and 1,2,3,5,6,7-Hexakis(3-hydroxy-3,3-diphenyl-2-propynyl)naphthalene.

SUSAN A. BOURNE[a,⋆], KATHERINE L. GIFFORD NASH[a] and FUMIO TODA[b]

[a]*Department of Chemistry, University of Cape Town, Rondebosch, 7701, South Africa*
[b]*Department of Applied Chemistry, Faculty of Engineering, Ehime University, Matsuyama 790, Japan*

(Received: 24 April 1998; in final form: 28 July 1998)

Abstract. The 2-hexanone inclusion compounds of hexakis(3-hydroxy-3,3-diphenyl-2-propynyl)benzene and 1,2,3,5,6,7-hexakis(3-hydroxy-3,3-diphenyl-2-propynyl)naphthalene have been prepared and characterised by single crystal X-ray diffraction and thermal analysis. The kinetic parameters and mechanisms for the desolvation reaction have also been determined for both compounds.

Key words: 2-hexanone inclusion compounds, hexapedal hosts, desolvation kinetics

Supplementary Data relating to this article are deposited with the British Library as Supplementary Publication No. SUP 82254 (49 pages).

1. Introduction

The three basic aspects of supramolecular chemistry include molecular recognition, supramolecular reactivity and catalysis and transport processes [1]. Molecular recognition involves chiefly the selective complexation of the host-guest type. A host that forms complexes of different stabilities with two similar guests is said to show molecular recognition and such selective complexation plays an essential role in the various aspects of supramolecular functions [2]. It has been observed that in order to achieve selectivity a host molecule must be rigid so as to allow a preorgan-

⋆ Author for correspondence.

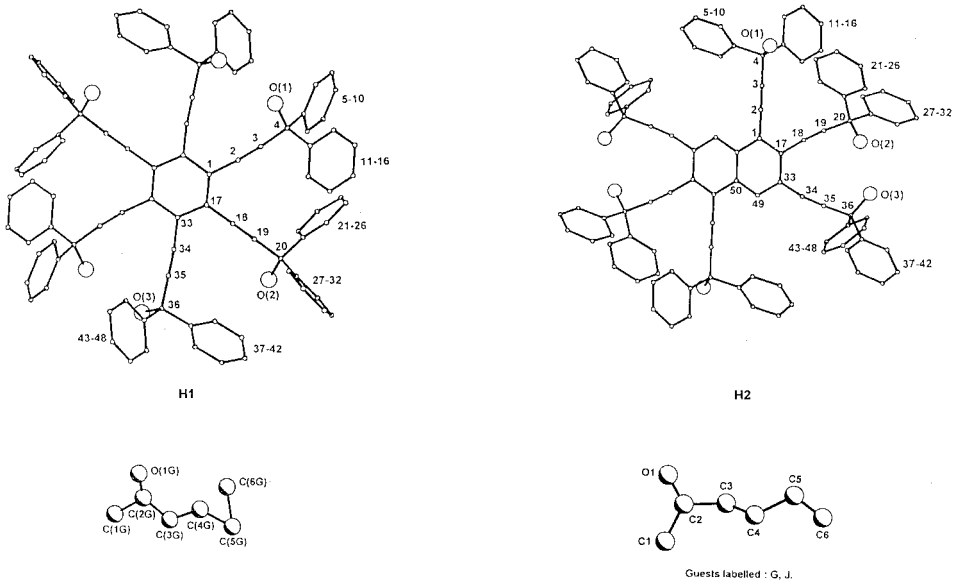

Scheme 1. Atomic labelling schemes used for **1** and **2**.

ised binding site which is complementary in size and polarity to a particular guest [3].

In recent years, we have studied a series of host compounds which fit the criteria above, and have, in addition, a relatively large number of hydrogen-bonding donor sites. Two such host compounds are hexakis(3-hydroxy-3,3-diphenyl-2-propynyl)benzene (**H1**), and 1,2,3,5,6,7-hexakis(3-hydroxy-3,3-diphenyl-2-propynyl)naphthalene (**H2**). **H1** includes a wide variety of guest molecules [4] and exhibits specific selectivity towards carbonyl-type oxygens over etheric oxygens [5]. **H2**, although similar in shape to **H1**, is a larger molecule and displays a preference for somewhat larger guests. Both **H1** and **H2** included 2-hexanone. This is interesting as inclusion compounds containing long-chain ketones are rarely reported. A search of the Cambridge Structural Database [6] reveals that, although *ca.* 20 structures with 2-butanone as guest have been reported, only one example of a 2-heptanone solvate is known [7], and there are no examples of 2-pentanone or 2-hexanone.

We report here the single crystal structures of the inclusion compounds of **H1** and **H2** with 2-hexanone as guest (**1**: **H1**: 2-hexanone, 1 : 2; **2** : **H2**: 2-hexanone, 1 : 4) as well as the results of kinetic studies on the thermal desolvation reactions of both compounds.

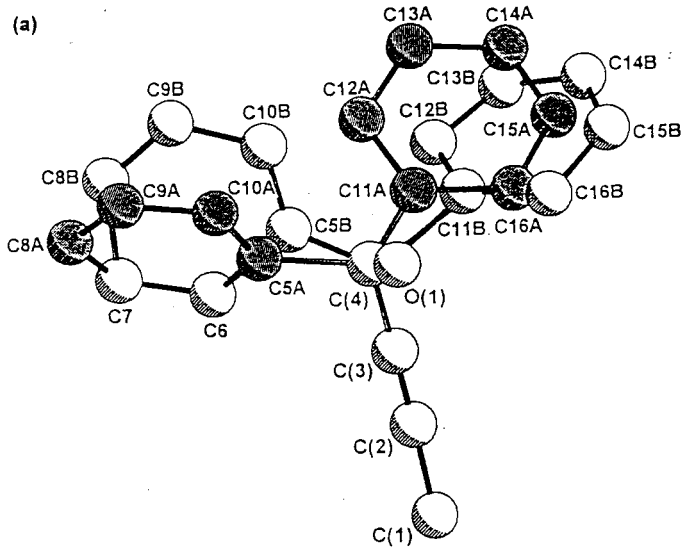

Figure 1. Disorder model in **2** for (a) host compound (**H2**), (b) guest G, and (c) guest J.

2. Experimental

2.1. CRYSTAL STRUCTURE DETERMINATION

The inclusion compounds **1** and **2** were obtained by dissolving the appropriate host compound in an excess of 2-hexanone. Slow evaporation at room temperature of the solutions yielded suitable single crystals for X-ray diffraction. In both cases

the crystals were unstable in air, and were mounted in flame sealed capillary tubes for data collection. Preliminary cell dimensions and space group symmetry were determined photographically. X-ray diffraction data were then measured on an Enraf-Nonius CAD4 diffractometer using graphite monochromated Mo K_α radiation (λ = 0.7107 Å) in ω-2θ scan mode. The data were collected at 223 K, in order to minimise thermal motion within the structure. Three reference reflections were monitored periodically to check orientation and crystal stability. The data reduction included correction for Lorentz and polarisation effects, but not for absorption.

The atomic labelling scheme used is shown in Scheme 1. Both the structures were solved by direct methods using SHELXS-86 [8], and refined by full matrix least-squares using SHELXL-93 [9], refining on F^2. In **1**, the host molecule lies on a centre of symmetry at ($\frac{1}{2}$, 0, $\frac{1}{2}$). All the host non-hydrogen atoms and guest oxygen atom were refined anisotropically. The guest carbons were refined isotropically because of their relatively high temperature factors. The hydroxyl hydrogens were located in the difference electron density map. H(1O) and H(2O) were allowed to refine independently with isotropic temperature factors, while H(3O), which was not involved in a hydrogen-bond, was refined with a temperature factor linked to O(3). The phenyl hydrogens were placed in geometrically calculated positions and refined with a common temperature factor. The guest hydrogens were omitted from the final model. A residual electron density of 0.96e $Å^{-3}$ is located close to the guest, but was not included in the final model. In **2**, the host lies on a centre of symmetry. All the non-hydrogen atoms were refined anisotropically. The hydroxyl hydrogens were located in the difference electron density maps and allowed to refine isotropically. The phenyl hydrogens were placed in geometrically calculated positions and refined with a common temperature factor. The guest hydrogens were omitted from the final model. Two of the phenyl rings on one of the legs of **H2**, C(5)–C(10) and C(11)–C(16), and both guests were found to be disordered. The disorder models are shown in Figure 1. Guest *G* was also refined with bond length restraints, to improve the geometry of the molecule. An extinction coefficient of 0.011(2) was applied to the data.

The crystal data and experimental conditions are listed in Table I. Fractional atomic coordinates are given in Table II. All the bond lengths and angles lie within expected ranges [10].

2.2. THERMAL ANALYSIS

Thermogravimetry (TG) and differential scanning calorimetry (DSC) were performed on a Perkin Elmer PC7 series system. The crystals were removed from their mother liquor, blotted dry and crushed before analysis. The TG and DSC runs were carried out on samples of 3–5 mg at a scan rate of 10 °C min^{-1}, over the temperature range 30–300 °C. The purge gas was dry nitrogen flowing at *ca.* 40 cm^3 min^{-1} for the TG experiments and *ca.* 30 cm^3 min^{-1} for the DSC experiments.

Table I. Crystal data and details of structure refinement

Parameter	**1**	**2**
Molecular formula	$C_{96}H_{66}O_6 \cdot 2C_6H_{12}O$	$C_{100}H_{68}O_6 \cdot 4C_6H_{12}O$
Molecular weight (g mol^{-1})	1515.89	1766.27
Crystal system	Triclinic	Triclinic
Space group	$P\bar{1}$	$P\bar{1}$
a (Å)	8.886(5)	8.539(1)
b (Å)	16.283(9)	16.907(3)
c (Å)	16.386(6)	18.907(3)
α (°)	117.26(3)	114.58(1)
β (°)	91.32(4)	97.65(1)
γ (°)	82.56(5)	92.90(1)
Volume (Å^3)	2088(2)	2443(1)
Z	1	1
Density calculated (g cm^{-3})	1.205	1.201
Density measured (g cm^{-3})	1.185	1.184
Linear absorption coefficient μ (mm^{-1})	0.075	0.075
F(000)	802	940
Colour	Pale yellow	Pale yellow
Data collection scan width (mm)	0.8 + 0.35 tan θ	0.8 + 0.35 tan θ
Vertical aperture (mm)	4	4
Aperture width (mm)	1.12 + 1.05 tan θ	1.12 + 1.05 tan θ
Size of crystal (mm)	0.25 × 0.35 × 0.45	0.41 × 0.44 × 0.44
Range scanned θ (°)	1–28	1–25
Range of indices h, k, l	−10, 10; −19, 17; 0, 19	−10, 10; −20, 18; 0, 22
Reflections measured	8009	8865
Unique reflections	7379	8579
Number of reflections observed with $I_{rel} > 2\sigma I_{rel}$	3405	5324
Decay of standard reflections (%)	1.0	−0.5
Final refinement		
R1 ($I_{rel} > 2\sigma I_{rel}$)	0.1043	0.0638
wR2 ($I_{rel} > 2\sigma I_{rel}$)	0.2872	0.1892
w*	a = 0.2096, b = 2.27	a = 0.1499, b = 1.54
S	1.030	0.949
Extinction coefficient	–	0.011(2)
Mean shift/esd	0.001	0.16
Max. height in difference Fourier map (eÅ^{-3})	0.967	0.416
Min. height in difference Fourier map (eÅ^{-3})	−0.633	−0.281

* $w = 1[\sigma^2(F_o^2) + (aP)^2 + bP]$ were $P = (\max(0, F_o^2) + F_c^2)/3$.

Table II. Atomic coordinates ($\times 10^4$) and equivalent isotropic displacement parameters ($Å^2 \times 10^3$)

	x	y	z	U(eq)
Compound 1				
C(1)	5073(7)	943(4)	5566(3)	30(1)
C(2)	5135(7)	1921(4)	6143(4)	32(1)
C(3)	5164(7)	2733(4)	6583(4)	36(2)
C(4)	5250(7)	3742(4)	7122(4)	34(1)
O(1)	4637(6)	4203(3)	6600(3)	42(1)
C(5)	4321(7)	4175(4)	8020(4)	33(1)
C(6)	4051(8)	5148(4)	8516(5)	48(2)
C(7)	3278(9)	5562(5)	9350(5)	57(2)
C(8)	2777(9)	5045(5)	9718(5)	57(2)
C(9)	3022(9)	4085(5)	9242(5)	52(2)
C(10)	3804(8)	3652(4)	8395(4)	43(2)
C(11)	6907(7)	3889(4)	7345(4)	37(2)
C(12)	7851(9)	3323(5)	7630(5)	50(2)
C(13)	9291(9)	3516(6)	7909(5)	56(2)
C(14)	9800(10)	4267(6)	7909(6)	67(2)
C(15)	8923(9)	4822(5)	7610(6)	63(2)
C(16)	7477(9)	4644(4)	7336(5)	49(2)
C(17)	5094(7)	605(4)	4602(4)	30(1)
C(18)	5187(7)	1248(4)	4245(4)	32(1)
C(19)	5300(7)	1868(4)	4060(4)	36(2)
C(20)	5351(7)	2716(4)	3942(4)	32(1)
O(2)	5980(6)	3391(3)	4760(3)	38(1)
C(21)	6296(7)	2521(4)	3092(4)	34(1)
C(22)	6589(8)	1636(5)	2372(5)	48(2)
C(23)	7339(9)	1494(6)	1567(5)	63(2)
C(24)	7790(9)	2231(7)	1501(5)	66(2)
C(25)	7516(9)	3114(6)	2220(5)	61(2)
C(26)	6751(8)	3254(5)	3007(5)	50(2)
C(27)	3754(7)	3134(4)	3874(4)	32(1)
C(28)	2732(8)	2573(4)	3312(4)	42(2)
C(29)	1299(8)	2932(5)	3225(5)	52(2)
C(30)	830(9)	3888(5)	3703(5)	56(2)
C(31)	1841(9)	4456(5)	4259(6)	58(2)
C(32)	3294(8)	4093(4)	4348(5)	45(2)
C(33)	5000(7)	−354(4)	4043(4)	33(1)
C(34)	4946(8)	−718(4)	3062(4)	36(2)
C(35)	4845(8)	−1083(4)	2245(4)	41(2)
C(36)	4519(8)	−1519(4)	1262(4)	39(2)
O(3)	3635(6)	−2267(3)	1077(3)	44(1)

Table II. Continued

	x	y	z	U(eq)
Compound 1 (continued)				
C(37)	5929(8)	−1909(4)	648(4)	39(2)
C(38)	5768(9)	−2438(4)	−302(4)	49(2)
C(39)	7026(10)	−2842(5)	−887(5)	58(2)
C(40)	8435(12)	−2737(6)	−557(7)	76(3)
C(41)	8615(11)	−2207(6)	378(7)	78(3)
C(42)	7354(9)	−1796(5)	971(5)	57(2)
C(43)	3478(8)	−780(4)	1110(4)	38(2)
C(44)	4105(10)	−119(5)	966(5)	54(2)
C(45)	3174(11)	593(5)	890(5)	62(2)
C(46)	1660(12)	647(6)	943(6)	72(3)
C(47)	1039(12)	−14(7)	1079(7)	90(3)
C(48)	1959(10)	−730(6)	1149(6)	69(2)
C(1G)	−1338(16)	6874(10)	4364(10)	124(4)
C(2G)	−78(12)	7388(7)	4877(7)	79(3)
O(1G)	1064(7)	6973(5)	4969(5)	92(2)
C(3G)	−652(31)	8417(20)	5243(21)	245(11)
C(4G)	250(22)	8965(15)	5890(14)	176(7)
C(5G)	−604(24)	10074(15)	6257(16)	192(8)
C(6G)	600(26)	10569(17)	6736(17)	211(9)
Compound 2				
O(1)	3877(3)	8629(1)	5984(1)	47(1)
O(2)	−187(3)	4525(2)	1444(1)	48(1)
O(3)	1281(3)	2076(2)	886(1)	49(1)
C(1)	3846(3)	5611(2)	4511(2)	26(1)
C(2)	3428(3)	6475(2)	4717(2)	32(1)
C(3)	3107(4)	7217(2)	4948(2)	38(1)
C(4)	2748(4)	8133(2)	5283(2)	53(1)
C(6)	−49(4)	7503(3)	5221(2)	53(1)
C(7)	−1561(5)	7566(4)	5432(3)	80(1)
C(5A)	1009(8)	8144(4)	5606(4)	34(1)
C(8A)	−1960(8)	8189(5)	6047(5)	61(2)
C(9A)	−793(8)	8881(5)	6472(4)	59(2)
C(10A)	690(7)	8861(4)	6254(4)	50(2)
C(5B)	1143(12)	8242(6)	5282(6)	41(2)
C(8B)	−1868(16)	8534(13)	5668(7)	95(5)
C(9B)	−884(18)	9189(10)	5676(7)	94(4)

Table II. Continued

	x	y	z	U(eq)
Compound 2 (continued)				
C(10B)	632(14)	9057(7)	5486(7)	76(3)
C(11A)	2774(12)	8549(5)	4792(5)	39(2)
C(12A)	1522(9)	8918(4)	4550(4)	63(2)
C(13A)	1707(12)	9322(5)	4047(5)	84(3)
C(14A)	3085(16)	9352(8)	3792(6)	87(3)
C(15A)	4358(16)	9001(7)	4030(7)	83(3)
C(16A)	4259(18)	8598(7)	4533(7)	55(4)
C(11B)	3410(18)	8490(7)	4593(7)	33(3)
C(12B)	2306(12)	8495(6)	3971(5)	54(2)
C(13B)	2849(22)	8802(10)	3465(8)	83(5)
C(14B)	4405(17)	9134(7)	3584(7)	70(3)
C(15B)	5471(19)	9095(8)	4173(8)	70(3)
C(16B)	5036(21)	8772(14)	4684(13)	67(6)
C(17)	3332(3)	4951(2)	3756(2)	27(1)
C(18)	2342(3)	5126(2)	3175(2)	32(1)
C(19)	1488(4)	5254(2)	2687(2)	38(1)
C(20)	387(4)	5367(2)	2070(2)	39(1)
C(21)	−1063(4)	5771(2)	2413(2)	41(1)
C(22)	−2542(5)	5329(3)	2136(3)	86(2)
C(23)	−3834(6)	5709(4)	2489(4)	127(3)
C(24)	−3618(5)	6515(4)	3101(3)	88(2)
C(25)	−2159(5)	6959(3)	3361(2)	73(1)
C(26)	−884(5)	6588(3)	3023(2)	70(1)
C(27)	1226(4)	5953(2)	1762(2)	43(1)
C(28)	721(5)	5850(3)	997(2)	57(1)
C(29)	1451(5)	6374(3)	708(3)	69(1)
C(30)	2676(5)	6994(3)	1166(3)	72(1)
C(31)	3172(5)	7115(4)	1929(3)	83(2)
C(32)	2447(5)	6592(3)	2220(2)	67(1)
C(33)	3768(3)	4089(2)	3566(2)	28(1)
C(34)	3287(3)	3399(2)	2785(2)	33(1)
C(35)	2961(4)	2797(2)	2149(2)	37(1)
C(36)	2670(4)	2025(2)	1373(2)	40(1)
C(37)	2362(4)	1191(2)	1489(2)	45(1)
C(38)	1125(5)	556(2)	1031(2)	55(1)
C(39)	942(6)	−213(2)	1124(3)	70(1)
C(40)	1953(7)	−352(3)	1669(3)	79(2)

Table II. Continued

	x	y	z	U(eq)
Compound 2 (continued)				
C(41)	3174(7)	284(3)	2129(3)	87(2)
C(42)	3375(6)	1055(3)	2045(2)	69(1)
C(43)	4133(4)	1970(2)	954(2)	40(1)
C(44)	4243(5)	1217(2)	297(2)	51(1)
C(45)	5536(5)	1148(2)	−87(2)	61(1)
C(46)	6728(5)	1831(3)	177(2)	59(1)
C(47)	6616(5)	2592(3)	823(2)	61(1)
C(48)	5320(4)	2663(2)	1212(2)	52(1)
C(49)	4676(3)	3917(2)	4130(2)	29(1)
C(50)	5204(3)	4568(2)	4901(2)	25(1)
C(1G)	3805(9)	4328(5)	204(7)	171(4)
C(2G)	2780(6)	3512(3)	49(3)	76(1)
O(1G)	1923(3)	3489(2)	496(2)	66(1)
C(3G)	2853(12)	2737(8)	−700(5)	173(4)
C(4GA)	1737(14)	2109(7)	−1068(7)	104(5)
C(4GB)	2297(21)	2438(11)	−1474(9)	114(6)
C(5G)	1925(18)	1449(8)	−2023(7)	202(6)
C(6GA)	3166(22)	1132(10)	−2175(10)	153(8)
C(6GB)	2067(31)	1342(18)	−2666(10)	192(12)
C(1JA)	1558(16)	8881(6)	7470(8)	94(5)
C(1JB)	2493(10)	8875(5)	8121(5)	67(3)
C(2J)	2180(6)	7961(3)	7329(3)	82(2)
O(1J)	3174(3)	7755(2)	6896(2)	62(1)
C(3J)	898(5)	7340(3)	7325(3)	66(1)
C(4JA)	1385(14)	6375(7)	7022(7)	53(3)
C(4JB)	756(10)	6467(7)	6612(8)	74(4)
C(5JA)	920(10)	5877(6)	6111(5)	49(3)
C(5JB)	1845(12)	5896(9)	6786(7)	75(3)
C(6J)	1446(7)	4945(3)	5907(4)	96(2)

2.3. KINETICS OF DESOLVATION

Powdered samples of uniform, small particle size, prepared by continuous stirring of 2-hexanone/host solutions until precipitation occured, were used for determining the kinetics of desolvation of **1** and **2**. The data for the kinetics of desolvation were obtained from isothermal TG experiments done at selected temperatures over the range in which the desolvation reaction proved to be isokinetic. A series of

Table III. Hydrogen bond data for **1**.

(D)onor	(A)cceptor	D—H (Å)	D···A (Å)	D—H···A (°)
O(1)	O(2)	1.00(8)	2.893(6)	162(6)
O(2)	O(1G)	0.87(8)	2.689(8)	156(8)

mass loss *vs.* time curves were obtained, which were then converted into fractional reaction (α) *vs.* time curves. Various appropriate kinetic models were fitted to the data [11]. The model chosen was the one which over the temperature range considered, most clearly approached linearity, over the largest α-range. The values of the rate constant (k) obtained at each temperature were used to produce an Arrhenius plot for the estimation of the activation energy of desolvation for each inclusion compound.

2.4. X-RAY POWDER DIFFRACTION

The powdered samples used for the determination of the kinetics of desolvation were packed in aluminium sample holders and the X-ray powder diffraction patterns measured using a Philips vertical goniometer with Ni filtered Cu K_α radiation (λ = 1.5418 Å) passed through 0.2° divergent and receiving slits, and a 1° antiscatter slit. The samples were scanned over the range 6-35° 2θ at intervals of 0.1° with a 2s count.

The X-ray diffraction powder patterns calculated from the single crystal structures were generated using LAZY-PULVERIX [12].

3. Results and Discussion

3.1. CRYSTAL AND MOLECULAR STRUCTURE

The molecular structure of **1** is shown in Figure 2(a). A cooperative hydrogen bonding scheme is observed between O(1), O(2) and O(1G), and the details are given in Table III. O(3) is not involved in any hydrogen bonding. Figure 3(a) shows the crystal packing of **1**. The host molecules stack in layers perpendicular to [010], with the central aromatic region parallel to the (100) planes. The guests are located in elongated cavities, which are situated between host layers, as shown in Figure 3(b).

The molecular structure of **2** is shown in Figure 2(b). Guest J is held in position by one hydrogen bond, while guest *G* is held in position by two, the details of which are given in Table IV. The crystal packing of **2** is shown in Figure 4(a). The host molecules pack in layers perpendicular to [001] with central aromatic regions approximately parallel to [101]. The guests are located in interconnecting cavities centred at x = 0.25 and x = 0.75. Guest J is located between adjacent host

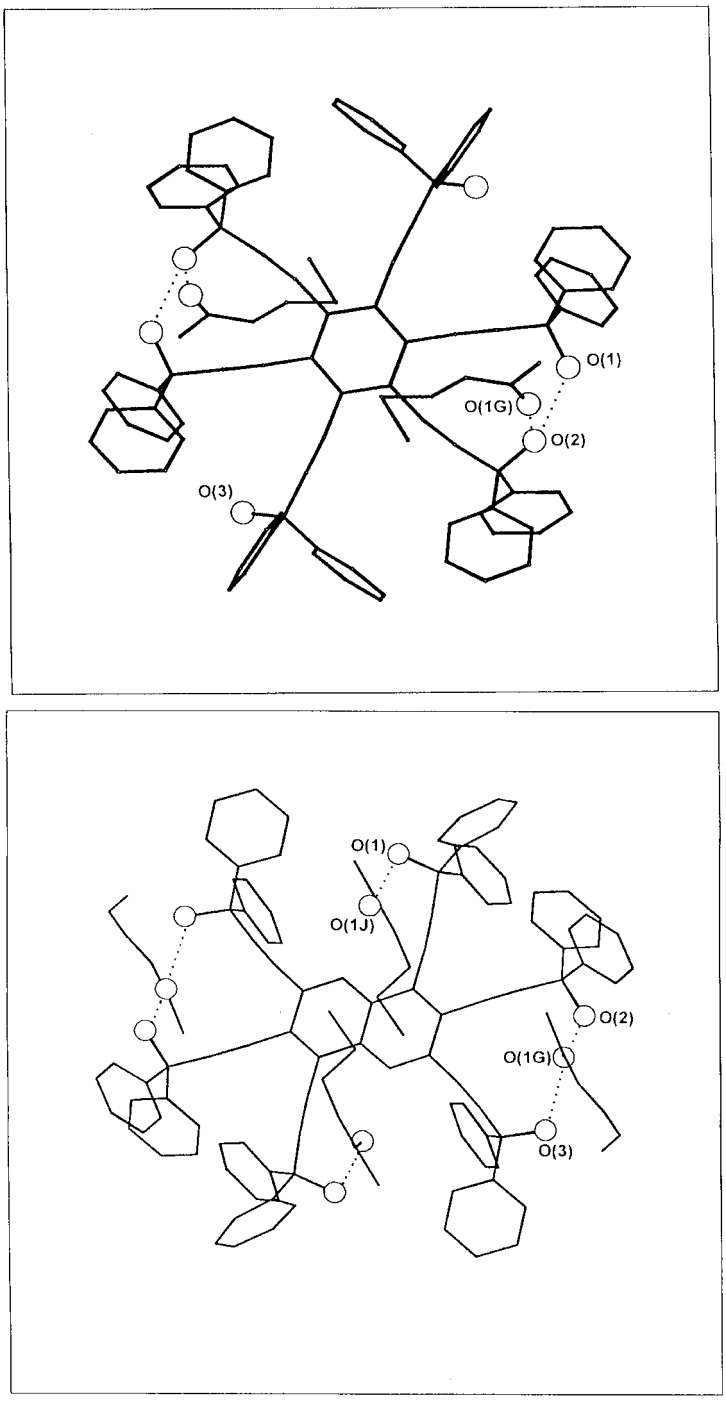

Figure 2. (a) Molecular structure of (a) **1** and (b) **2** (the hydrogen atoms are omitted for clarity and the hydrogen bonds are indicated by dotted lines).

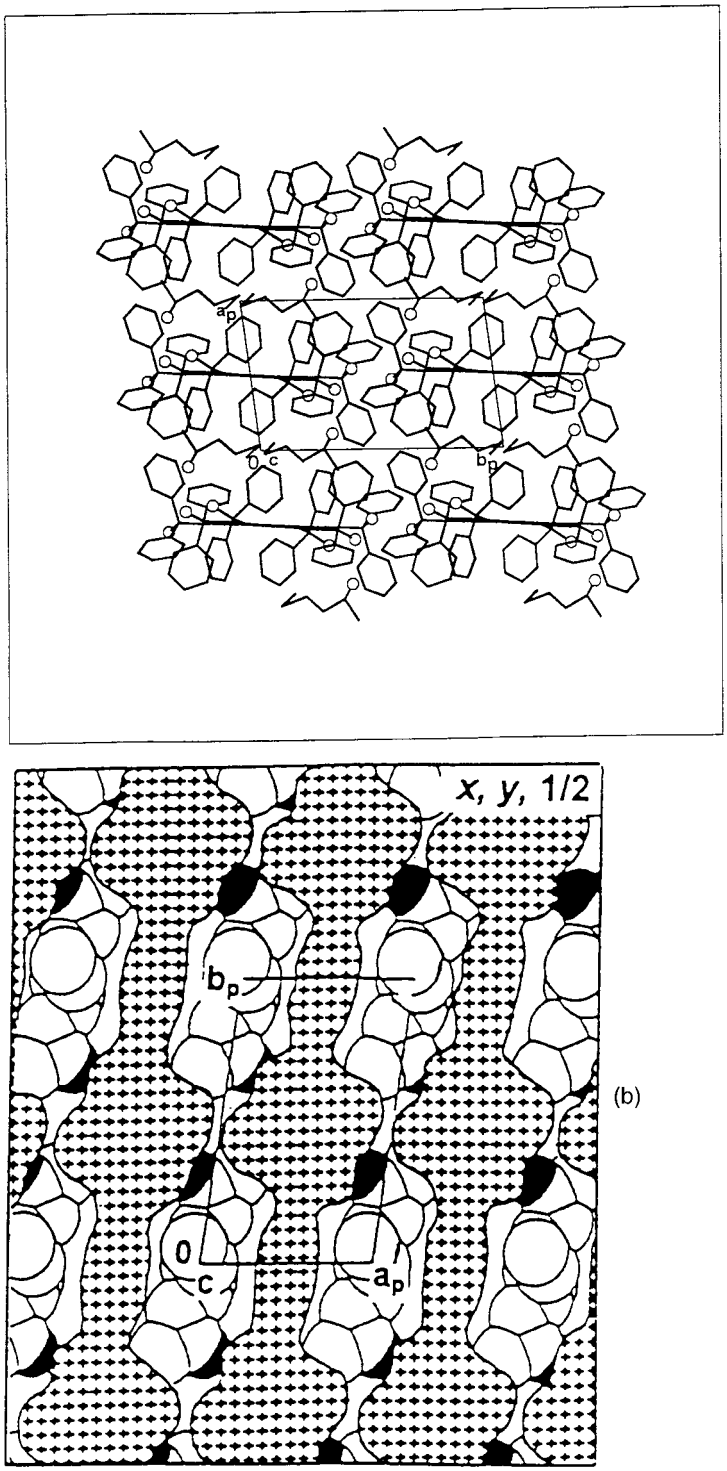

Figure 3. (a) Crystal packing in **1**, viewed down [001]. (b) Cross section of **1**. Hatched areas represent regions occupied by host. Guest molecules are shown (with oxygens shaded) in the cavities.

Table IV. Hydrogen bond data for **2**.

(D)onor	(A)cceptor	D—H (Å)	D···A (Å)	D—H···A (°)
O(1)	O(1J)	0.97(5)	2.797(4)	168(4)
O(2)	O(1G)	0.86(4)	2.845(4)	168(4)
O(3)	O(1G)	0.92(5)	2.827(4)	171(4)

molecules, above and below the central aromatic region, while guest *G* is located in the area between the layers of host molecules, in between the interlinking phenyl groups (see Figure 4(b)). The 2-hexanone molecules are in the extended, staggered conformation.

3.2. THERMAL ANALYSIS

Figure 5 shows the thermograms obtained for **1** and **2**. TG was used to confirm the host to guest ratios modelled in the crystal structures. For **1**, the TG curve shows a single step guest loss corresponding to a 1 : 2 stoichiometry (calculated mass loss: 13.2%, observed mass loss: 12.7%). The DSC trace shows a broad double endotherm at *ca.* 99°C, corresponding to guest loss and structural collapse of the host framework to that of the uncomplexed host framework. A sharper endotherm at 263 °C corresponds to the melt of the host, which then decomposes. For **2**, a rapid single step guest loss is also observed. The mass loss observed confirms the host to guest ratio of 1 : 4 modelled in the crystal structure (observed mass loss: 22.7%, expected mass loss: 21.8%). The DSC trace comprises a sharp endotherm at 74 °C, with is followed by a diffuse step in the baseline. The trace then shows two endotherms at 234 °C and 256 °C. The host framework of the inclusion compound may collapse into that of a polymorph of the uncomplexed host, which converts at 234 °C into that of another form of the uncomplexed host. This form then melts and decomposes at 256 °C.

3.3. KINETICS OF DESOLVATION

Data for the kinetics of desolvation were obtained from isothermal experiments carried out at temperature intervals of 2–3 °C over the temperature range 80–100 °C for **1**, and 55–75 °C for **2**. An example of the α-time curves obtained for **1** and for **2** are shown in Figure 6. For **1**, the curves are sigmoidal in shape, consisting of an induction period, an acceleratory period and a deceleratory period. The Avrami-Erofeev (A2) equation, derived to model two-dimensional nucleation and growth of the product phase [11], fits the data over the α-range 0.05–0.95, and an activation energy of 264(3) kJ mol^{-1} was obtained. The semilogarithmic plot of ln k vs. 1/T is shown in Figure 7(a). For **2**, the curves are deceleratory, and the best-fit kinetic

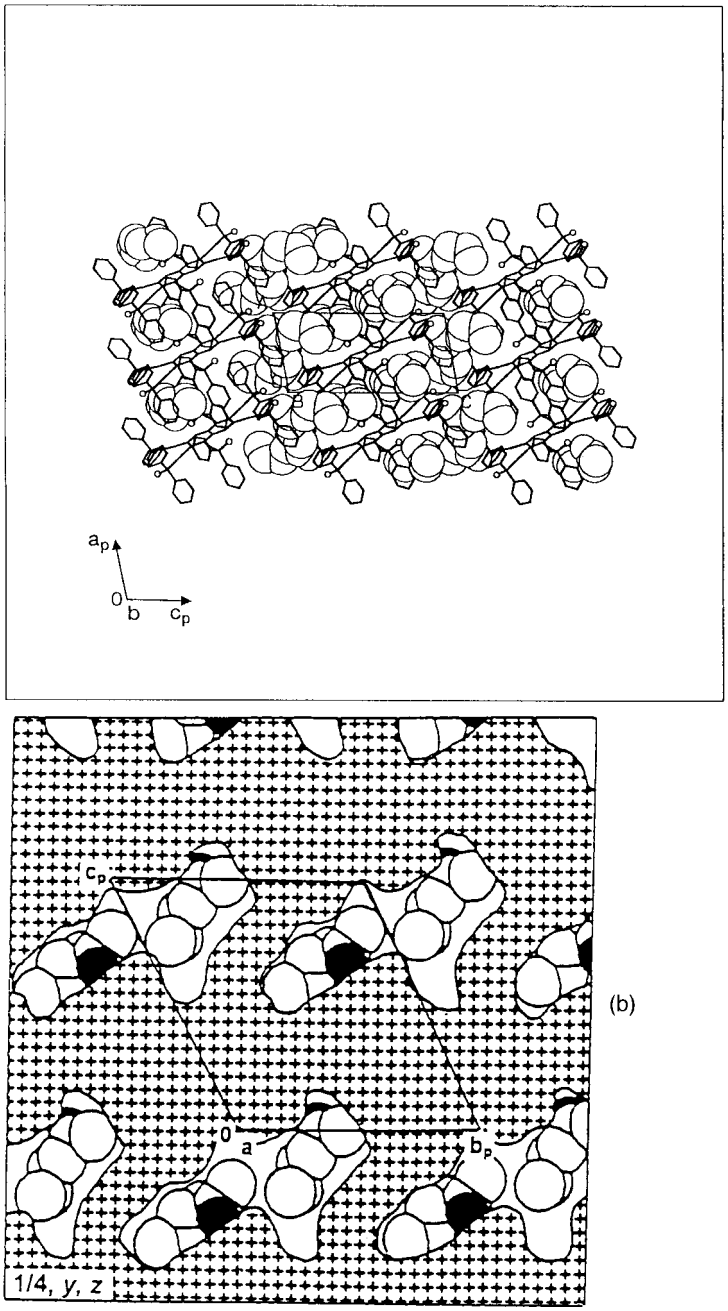

Figure 4. (a) Crystal packing in **2**, viewed down [010]. For clarity, guests are shown with van der Waals radii while hosts are shown in stick form. (b) Cross section of **2**. The hatched region is that occupied by host molecules, and the guests are shown in the cavities (with oxygens shaded).

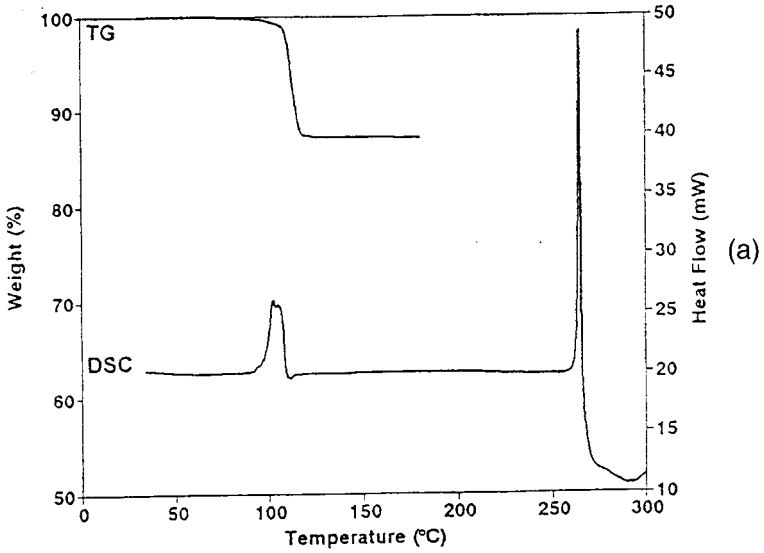

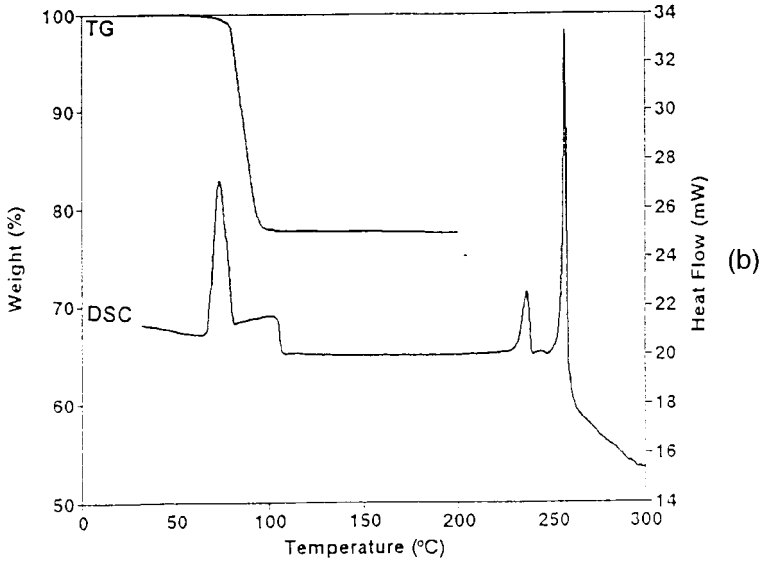

Figure 5. Thermograms of (a) **1** and (b) **2**.

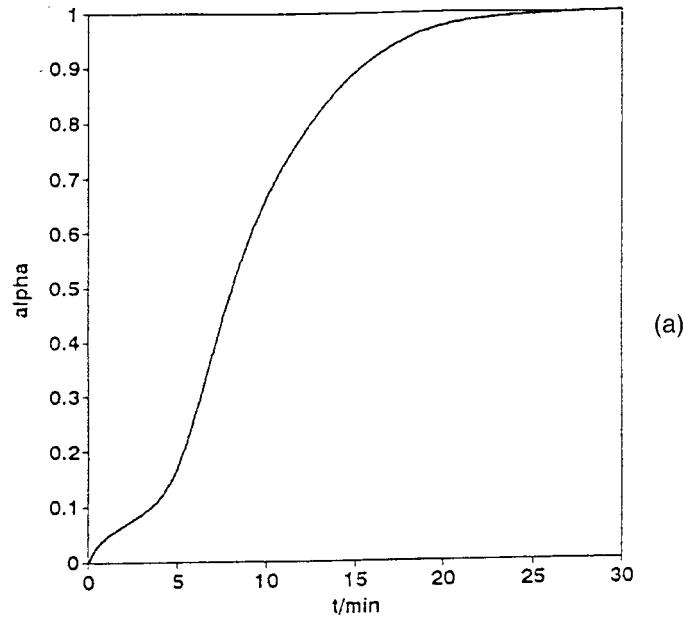

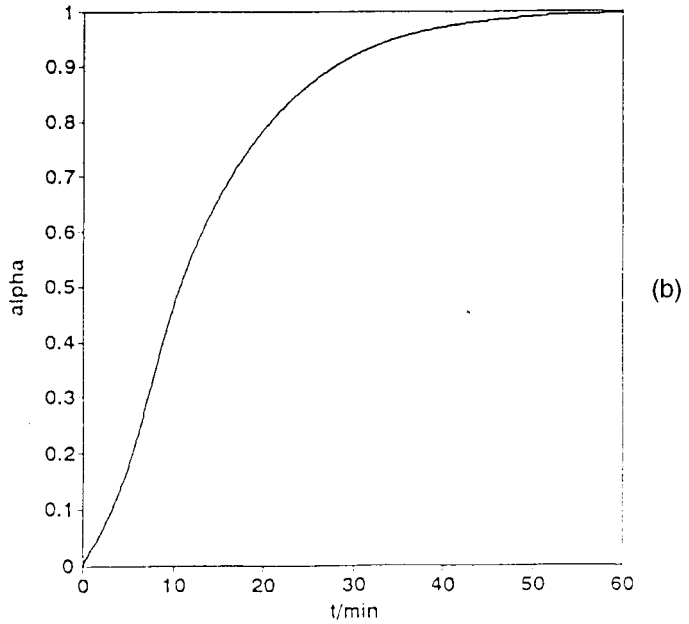

Figure 6. An example of an α vs. time curve obtained for (a) **1** and (b) **2**.

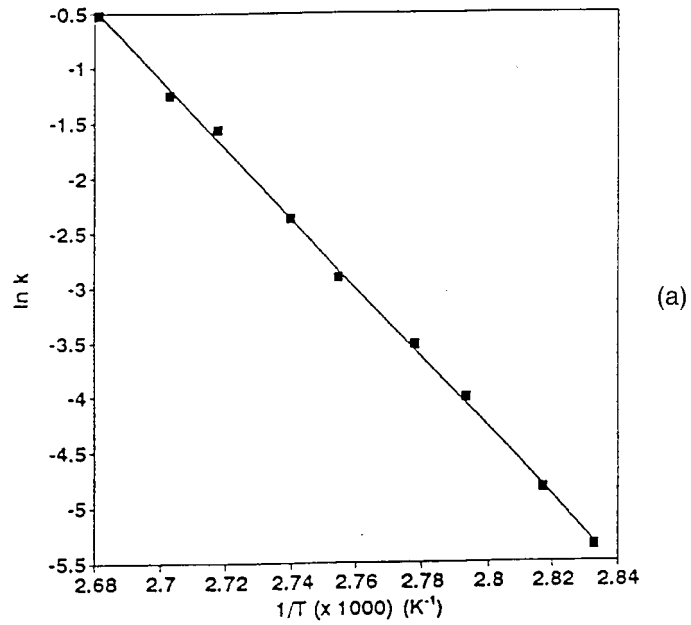

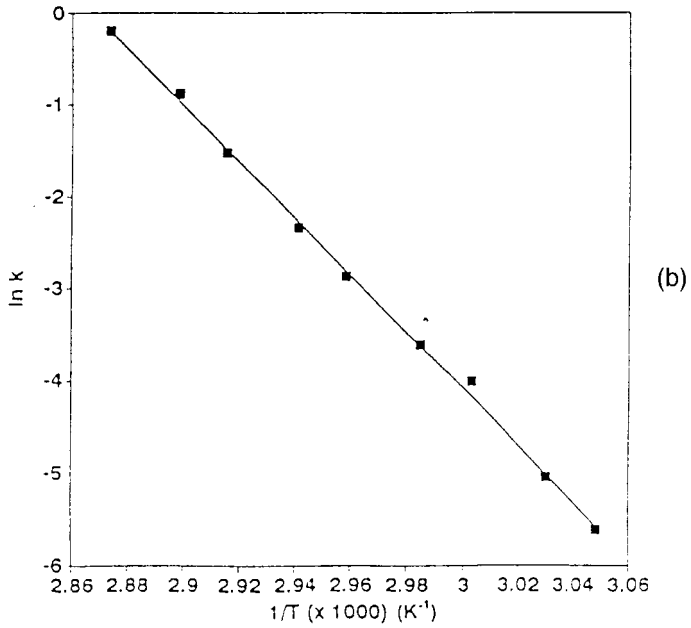

Figure 7. Arrhenius plot for the desolvation of (a) **1** and (b) **2**. The slope of this plot gives the value of the activation energy for the desolvation process.

model was found to be the first order reaction mechanism [11] (α-range 0.05–0.95). The semilogarithmic plot of ln k vs. 1/T is shown in Figure 7(b), and yields an activation energy of 256(4) kJ mol^{-1}.

3.4. X-RAY POWDER DIFFRACTION

X-ray powder diffraction was used to confirm that for each of the inclusion compounds, the single crystals and powdered sample had the same structure. The experimental diffraction patterns of the powdered samples were compared with the powder diffraction patterns calculated from the crystal structure. For each inclusion compound, the two patterns were identical. The powder diffraction patterns of the desolvated material for **1** and **2** were also collected, and clearly show that the inclusion compounds undergo a phase change on desolvation to that of the uncomplexed host material.

4. Conclusion

We have reported the structures of two inclusion compounds of related multipedal hosts with 2-hexanone as guest. In both, the hexanone adopts an extended conformation and is hydrogen bonded to the host through its carbonyl oxygen. There are no other host-guest interactions. The activation energy for the desolvation reactions are relatively high in comparison to those reported for other organic host compounds (generally in the range 50–200 kJ mol^{-1}) [13]. The hexanone guests are found in cavities which is usually associated with activation energies in the higher region of this range.

Acknowledgements

We thank the University of Cape Town and the Foundation for Research Development for financial assistance.

References

1. J-M. Lehn: in H-J. Schneider and H. Dürr (eds.), *Frontiers in Supramolecular Organic Chemistry and Photochemistry*, VCH Publishers, Weinheim, New York (1991).
2. Y. Aoyama: in V. Balzani and L. De Cola (eds.), *Supramolecular Chemistry*, Kluwer Publishers, Dordrecht (1992).
3. E. Weber: in J. L. Atwood, J. E. D. Davies and D. D. MacNicol (eds.), *Inclusion Compounds*, Vol. 4, Oxford University Press (1991).
4. (a) S. A. Bourne, M. R. Caira, L. R. Nassimbeni, M. Sakamoto, K. Tanaka, F. Toda, *J. Chem. Soc., Perkin Trans. 2*, 1899 (1991). (b) S. A. Bourne, K. L. Gifford Nash, F. Toda, *J. Chem. Soc., Perkin Trans. 2*, 2145 (1996).
5. S. A. Bourne, K. L. Gifford Nash, F. Toda, *Supramol. Chem.* **8**, 137 (1997).
6. Cambridge Structural Database, version 5.13, Cambridge Crystallographic Data Centre, Cambridge, United Kingdom, (October 1997).

7. R. Popovitz-Biro, C. P. Tang, H. C. Chang, M. Lahav, L. Leiserowitz, *J. Am. Chem. Soc.* **107**, 4043 (1985).
8. G. M. Sheldrick, *Acta Crystallogr., Sect. A.* **46**, 467 (1990).
9. G. M. Sheldrick, SHELXL-93, University of Göttingen (1993).
10. F. H. Allen, O. Kennard, D. G. Watson, L. Brammer, A. G. Orpen, R. Taylor, *J. Chem Soc., Perkin Trans. 2*, S1 (1987).
11. M. E. Brown, *Introduction to Thermal Analysis*, Chapman and Hall, London (1988).
12. K. Yvon, W. Jeitschko, E. Parthé, *J. Appl. Crystallogr.* **10**, 73 (1977).
13. K. L. Gifford Nash, *Ph.D. Thesis*, University of Cape Town (1997).